Structural and magnetic transitions in the crystalline approximant Cd_6Sm

R. Tamura,[1,*] Y. Muro,[2] T. Hiroto,[1] H. Yaguchi,[3] G. Beutier,[4] and T. Takabatake[2,5]

[1]*Department of Materials Science and Technology, Tokyo University of Science, 2641 Yamazaki, Noda, Chiba 278-8510, Japan*

[2]*Department of Quantum Matter, AdSM, Hiroshima University, Higashi-Hiroshima 739-8530, Japan*

[3]*Department of Physics, Tokyo University of Science, Noda 278-8510, Japan*

[4]*SIMaP, Grenoble-INP-CNRS-UJF, BP 75, 38402 Saint-Martin d'Hères cedex, France*

[5]*Institute for Advanced Materials Research, Hiroshima University, Higashi-Hiroshima 739-8530, Japan*

(Received 13 March 2011; revised manuscript received 26 December 2011; published 20 January 2012)

Electrical resistivity, specific heat, magnetic susceptibility, and magnetization of the crystalline approximant Cd_6Sm are investigated in a temperature range 1.8−300 K. Both structural and magnetic transitions are clearly evidenced. A sharp structural phase transition is observed at $T_c = 179$ K in the electrical resistivity as well as in the specific heat, which is attributed to orientational ordering of the Cd_4 tetrahedron located at the center of the icosahedral cluster. In addition, three successive magnetic transitions are found at $T_{M1} = 12.5$, $T_{M2} = 10.2$, and $T_{M3} = 6.5$ K. The anomaly at T_{M1} is attributed to an antiferromagnetic transition, whereas those at T_{M2} and T_{M3} are to ferrimagnetic transitions. The observation of the ferrimagnetic orders indicates that (pseudo) icosahedra made of localized Sm spins have a nonzero net magnetic moment, and the moments of the magnetic clusters form a long-range magnetic order.

DOI: 10.1103/PhysRevB.85.014203 PACS number(s): 61.44.Br, 64.70.K−, 75.50.Kj

I. INTRODUCTION

Cd_6Sm,[1] crystalline approximant, one of a series of isostructural Cd_6M(M = Ca, Sr, Y, Ce, Pr, Nd, Sm, Eu, Gd, Tb, Dy, Ho, Er, Tm, Yb, Lu) compounds,[2,3] is a *bcc* crystal [space group $Im\bar{3}$,$a = 15.589(3)$Å] composed of so-called Tsai-type icosahedral clusters. A Tsai-type cluster, which is regarded as the building block of the stable binary quasicrystals, $Cd_{5.7}Yb$[4] and $Cd_{5.7}Ca$,[5] is made of four successive shells: the first shell is a dodecahedron composed of 20 Cd atoms, the second shell an icosahedron of 12 M atoms, the third shell an icosidodecahedron of 30 Cd atoms, and the outermost shell a defect rhombic triacontahedron of 60 Cd atoms.[2] At the center of the Tsai-type cluster is located a Cd_4 tetrahedron, which is orientationally disordered at room temperature.

From an experimental point of view, the binary Cd_6M approximants are of particular interest because they have no chemical disorder among the constituent elements: M atoms occupy a single crystallographic site with full occupancy at room temperature, and the remaining sites are exclusively occupied by Cd atoms.[2] This structural property allows us to prepare a specimen of high structural quality with no chemical disorder, and thus one may expect that unique physical properties intrinsic to the icosahedral cluster or to an aggregate of the clusters can be obtained in the binary approximants.

Concerning the structural property of the Cd_6M compounds, a new kind of structural phase transition was reported in Cd_6M (M = Yb, Ca, Y, Ce, and Eu)[6–10] as well as in isostructural Zn_6Sc,[11] which has been interpreted as an order-disorder transition with respect to the orientation of the $Cd_4(Zn_4)$ tetrahedron at the center of the Tsai-type cluster.[12,13] Therefore, it is of interest whether such a structural transition is a common phenomenon over all the Cd_6M compounds having the same Tsai-type clusters and what the low-temperature superstructures for a series of the rare-earth (RE) elements are. One major problem that has been encountered through this research exists in the difficulty in the determination of the superstructure since the low-temperature phase is composed of small domains of ∼100 nm.[14] Moreover, there is also a difficulty in the determination of the space group solely by x-ray diffraction when the existence of the inversion symmetry needs to be verified, as in the cases of Cd_6Ca and Zn_6Sc. Concerning the latter point, Nishimoto *et al.* have recently determined the space group of the low-temperature Cd_6Sm by a convergent electron diffraction technique,[15] which has motivated the present work on Cd_6Sm since it allows us to discuss both the structural and the magnetic transitions in terms of the low-temperature superstructure model.

The Cd_6M compounds are also of interest from a viewpoint of their magnetic properties since most of them contain a RE element, providing a new type of spin system where localized RE spins sit on the vertices of a (pseudo)icosahedron, which packs into a chemical *bcc* lattice. With respect to the interaction between the M ions, one finds that the nearest neighbours are not M-M pairs but that the M ions are separated from the nearest ones by ∼0.6 nm, indicating that the magnetic interaction between the M ions is mediated by conduction electrons, i.e., RKKY interaction. Recently, a long-range magnetic order has been reported in Cd_6Tb showing that localized Tb spins are antiferromagnetically ordered at low temperatures.[16] Therefore, it has now become an important issue to clarify what type of magnetic order occurs for the series of Cd_6M with different RE elements having different magnetic moments. In this paper we report both structural and magnetic transitions of Cd_6Sm in terms of electrical, thermal, and magnetic properties and discuss the transition phenomena based on the low-temperature superstructure.

II. EXPERIMENTAL

Single grains were prepared by a self-flux method by melting high-purity elements of Cd(99.9999wt%) and Sm(99.9wt%) of a 9:1 atomic ratio at 993 K for 24 h in an alumina crucible sealed inside a quartz tube, followed by slow cooling at the rate of −2 K/h down to 773 K. Then, the

remaining Cd melt was removed by means of a centrifuge, and the alloys were subsequently annealed at 873 K for 50 h to improve the sample homogeneity as well as to reduce point defects. Single grains of mm size with well defined facets of {100} and {110} planes are obtained. The phase purity of the samples was examined by powder x-ray diffraction as well as by transmission electron microscopy. Electrical resistivity measurements were performed by a four-probe method using an ac-resistance bridge for both cooling and heating processes in a range 2−300 K. Magnetic properties were measured from 1.8 to 300 K by using a SQUID magnet meter (Quantum Design, MPMS) in magnetic fields up to 50 000 Oe, and specific heat was measured in a relaxation method from 1.8 to 300 K.

III. RESULTS AND DISCUSSION

A. Electrical and thermal measurements

Figure 1(a) shows electrical resistivity ρ of Cd_6Sm as a function of temperature measured on heating from 2 to 300 K together with its temperature derivative $d\rho/dT$. The resistivity exhibits a positive temperature coefficient in the entire temperature region showing a metallic nature of Cd_6Sm. An extraordinary sharp stepwise anomaly is noticed at T_c = 179 K, suggesting an occurrence of a phase transition. Such a sharp anomaly is comparable to that observed in Zn_6Sc of the highest perfection.[17] Figure 2(a) magnifies the ρ-T curve of Cd_6Sm below 30 K, and the inset shows the ρ-T curves between 4 and 13 K measured for both the cooling and heating processes. A significant reduction of the resistivity is observed with an onset temperature of ∼10.2 K, and in addition a small anomaly is noticed at 6.5 K. The anomaly at 6.5 K accompanies slight hysteresis between the cooling and the heating curves, as seen from the inset. The latter two anomalies will be understood as a result of loss of electron scattering due to successive magnetic transitions.

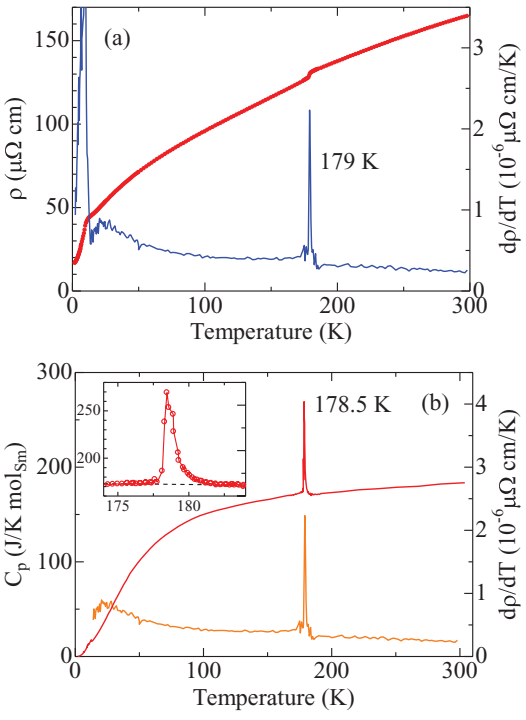

FIG. 1. (Color online) (a) Electrical resistivity ρ (solid circles, red) and its temperature derivative $d\rho/dT$ (solid line, blue) of Cd_6Sm as a function of temperature from 1.8 to 300 K. (b) Specific heat C_p (top, solid line, red) of Cd_6Sm as a function of temperature between 2 and 300 K. The $d\rho/dT$-T curve (bottom, solid line, orange) is replotted for a comparison. The inset magnifies the peak at 178.5 K, and the broken line represents the background assumed for the estimation of the transition entropy.

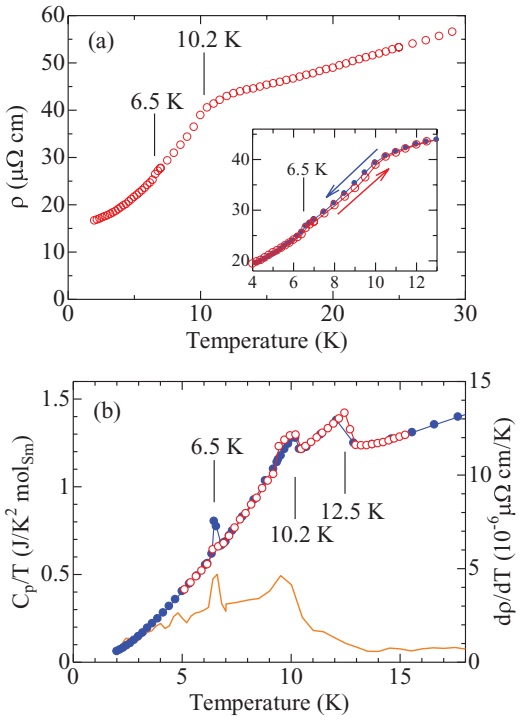

FIG. 2. (Color online) (a) Electrical resistivity ρ (open circles, red) of Cd_6Sm below 30 K. The inset shows $\rho - T$ curves for both cooling (solid circles, blue) and heating (open circles, red) runs. Slight hysteresis is noticed for the anomaly at 6.5 K as seen in the inset. (b) Specific heat divided by temperature C_p/T of Cd_6Sm plotted as a function of temperature between 2 and 18 K measured with cooling (solid circles, blue) and heating (open circles, red) sequences. The $d\rho/dT$-T curve (solid line, orange) is replotted for a comparison.

Figure 1(b) shows specific heat C_p of Cd_6Sm as a function of temperature between 2 and 300 K together with the $d\rho/dT$-T curve. The specific heat also displays a sharp peak at 178.5 K with a very narrow peak width of ∼2 K and a small tail above T_c. The peak temperature corresponds exactly to the temperature of the resistivity anomaly at 179 K showing that the resistivity anomaly is caused by a phase transition. Concerning the low-temperature phase, selected area electron-diffraction patterns reveal superlattice reflections along a <110> axis below T_c,[15] indicating that the periodicity is doubled along a <110> direction due to the structural transition at T_c.

B. Structural transition

The observed salient peak in the C_p-T curve of Cd_6Sm suggests that the phase transition is of an order-disorder type and is readily attributed to orientational ordering of the Cd_4 tetrahedron at the center of the Tsai-type cluster as in the cases

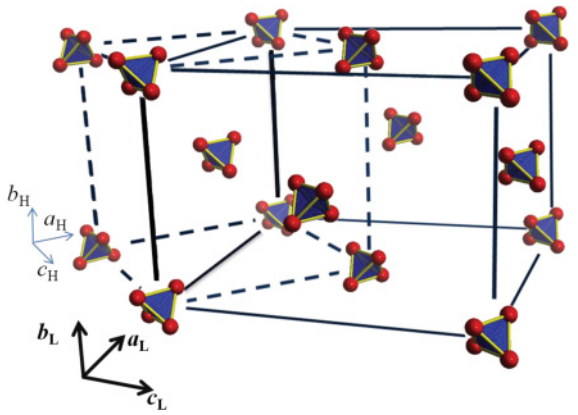

FIG. 3. (Color online) Schematic illustration of the low-temperature unit cell (space group $C2/c$) of Cd_6Sm with respect to the orientations of the central tetrahedra. The broken lines represent the unit cell of the high-temperature *bcc* lattice.

of isostructural Cd_6Ca[12] and Zn_6Sc.[13] Nishimoto *et al.* have recently determined the space group of Cd_6Sm to be $C2/c$ below T_c by a convergent electron-diffraction technique.[15] We note that $C2/c$ is a subgroup of the space group ($Im\bar{3}$) of the high-temperature phase, and the phase transition is associated with a single irreducible representation N_1^- (see Ref. 12) of a small group G_k with $k = (\frac{\pi}{a},0,\frac{\pi}{a})$ satisfying a condition of the continuous transition. The obtained space group $C2/c$ means that a twofold axis of the Cd_4 tetrahedra is parallel to the b-axis and two orientations are alternatively repeated along a [101] direction, i.e., $[001]_L$ direction of the $C2/c$ lattice, below T_c as schematically illustrated in Fig. 3. The narrow peak width of the peak in the C_p-T curve implies that the long-range orientational order develops very rapidly (in terms of temperature) within a narrow temperature region of ~2 K. On the other hand, the small tail observed above T_c suggests the existence of a short-range orientational order.

In order-disorder transitions, the transition entropy is associated with the number of possible configurations above T_c. From the C_p-T curve the transition entropy S is estimated by $S = \int \frac{C_p}{T} dT$. The obtained entropy is $S_{obs} = 0.792k_B$ per icosahedral cluster, which gives 2.21 states per cluster above T_c. The reported electron distribution of Cd_6Sm[2] suggests that the four Cd atoms at the center of the cluster are located near the mid-edge positions of a cube, cube octahedron sites. If we allow off-edge positions for each tetrahedron to be located, a twofold axis of the tetrahedron is lost, which is inconsistent with the obtained point group $2/m$. On the other hand, when a tetrahedron is placed on the edges of the cube, the number of possible states is either 24 or 12: 24 for off-mid edge and 12 for mid-edge positions. Hence the discrepancy of the transition entropy would become much bigger for the former case. For this reason it is most plausible that the tetrahedra occupy the mid-edge positions of the cube, and the observed deviation from the mid-edge positions in the electron distribution is due to thermal vibration of the tetrahedron, which is indistinguishable from static disorders by x-ray experiments. Thus, the number of the possible orientations for each Cd_4 tetrahedron is expected to be six above T_c, which predicts a transition entropy of $k_B\ln 6 (=1.79k_B)$ per icosahedral cluster. The experimental value is comparable to but much smaller than the expected one. The fact that the experimental value is comparable to the expected one supports the interpretation of the phase transition with respect to orientational ordering of the Cd_4 tetrahedra. On the other hand, for the discrepancy, we note the following two cases as possible origins. One is a contribution from the formation enthalpy of domain boundaries, which is not taken into account in the previous argument. Since the Laue groups of the high and the low temperature phases are $m\bar{3}$ (order 24) and $2/m$ (order 4), respectively, six different domains are formed below T_c, which will cost a formation energy reducing the transition heat. The other possibility that is neglected in the previous argument is the existence of disordered Cd_4 tetrahedra even below T_c, which are kinetically frozen by structural disorders such as point defects. In the case of Zn_6Sc, the experimental value of the transition entropy is found to be very sensitive to the sample preparation condition and well correlated with the residual resistivity value,[17] which clearly indicates that structural defects such as point defects locally suppress orientational ordering of the Zn_4 tetrahedron in the case of Zn_6Sc. These facts allow us to conjecture that the

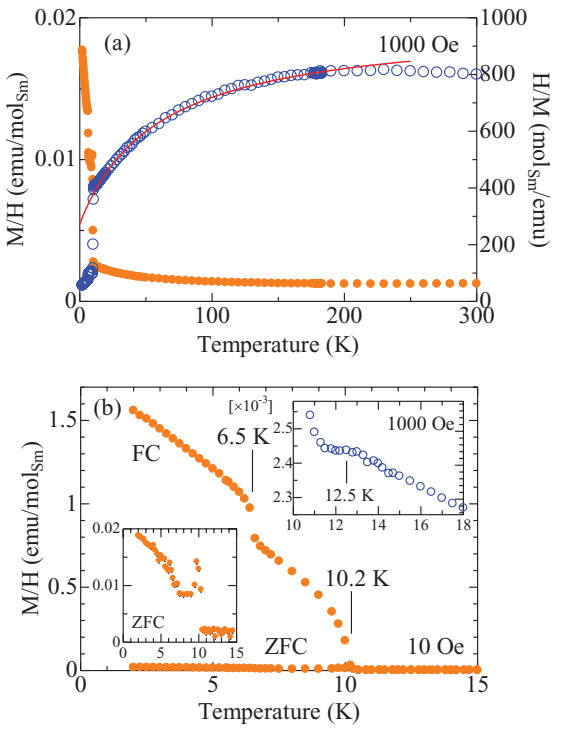

FIG. 4. (Color online) (a) Magnetic susceptibility M/H (solid circles, orange) and inverse susceptibility H/M (open circles, blue) of Cd_6Sm measured with a magnetic field of 1000 Oe. The solid line (red) represents a least-square fit to the Curie-Weiss law incorporating a temperature independent Van Vleck contribution in a temperature range 15−200 K. (b) Magnetic susceptibility M/H of Cd_6Sm in a low temperature region between 1.8 and 15 K measured with a magnetic field of 10 Oe. Field-cooled (FC) and zero field-cooled (ZFC) magnetic susceptibilities are shown in the figure. The left inset shows a zoomed ZFC curve, and the right inset shows the M/H-T curve of Cd_6Sm measured with a magnetic field of 1000 Oe, where an inflection due to an antiferromagnetic transition is noticed at ~12.5 K.

observed transition entropy is always smaller than the expected value for the present phase transition. Thus, we can reasonably exclude the case of two random orientations above T_c from the obtained states, i.e., 2.21 states per cluster, which is consistent with the reported electron density distribution of the Cd_4 tetrahedon at room temperature where the Cd atoms occupy the mid-edge positions of the cube, not its vertices.[2]

C. Magnetic transitions

Figure 2(b) shows the C_p/T-T curve in a low temperature region below 18 K. Three anomalies are noticed at $T_{M1} = 12.5$, $T_{M2} = 10.2$, and $T_{M3} = 6.5$ K, showing an occurrence of successive phase transitions. Among them, the anomaly at T_{M3} corresponds exactly to the stepwise anomaly observed at 6.5 K in the resistivity and the one at T_{M2} corresponds to the onset temperature of the significant drop of the resistivity. Hysteresis is also noticed for the 6.5 K-anomaly between the cooling (solid circles) and heating curves (open circles), consistent with the resistivity, indicating that the phase transition at T_{M3} is of a first order.

Figures 4(a) and 4(b) show magnetic susceptibility of Cd_6Sm measured at 1000 and 10 Oe in a temperature range between 1.8 and 300 K and between 1.8 and 15 K, respectively. No magnetic anomaly is observed at the structural phase transition, i.e., at $T_c = 179$ K. As seen from Fig. 4(a), the susceptibility of Cd_6Sm does not obey the Curie-Weiss law, which is rather a typical behaviour of Sm^{3+} ions due to the small energy difference between the Hund's rule ground state $J = 5/2$ multiplet and the first excited $J = 7/2$ multiplet.[18] Since higher-level multiplets may also contribute to the susceptibility at elevated temperatures, we fitted the susceptibility data in a lower temperature range between 15 and 200 K by the following expression, which incorporates the Curie-Weiss law a temperature-independent Van Vleck term due to thermal population of the first excited multiplet ($J = 7/2$)

$$\chi(T) = \left(\frac{N_A}{k_B}\right)\left[\frac{\mu_{\rm eff}^2}{3(T-\Theta)} + \frac{\mu_B^2}{\delta}\right],$$

where N_A is Avogadro's number, $\mu_{\rm eff}$ is the effective magnetic moment, Θ is the Curie-Weiss temperature, μ_B is the Bohr magneton, and $\delta = 7\Delta/20$ where Δ is the energy difference in units of K between the $J = 5/2$ and $J = 7/2$ multiplets.[19] The result of a least square fit to the modified Curie-Weiss law is satisfactory and the parameters obtained from the best fit are $\mu_{\rm eff} = 0.588(7)\mu_B$, $\Theta = -16(4)$K, and $\delta = 368(4)$ K[$\Delta = 1052(11)$ K]. The effective magnetic moment $\mu_{\rm eff}$ is somewhat smaller than the theoretical value ($0.85\mu_B$) of the $J = 5/2$ ground state of the Sm^{3+} free ion. The negative Θ value means that major interaction between spins is antiferromagnetic in the paramagnetic state. The energy difference between $J = 5/2$ and $J = 7/2$ multiplets is also smaller than the value ($\Delta \sim 1500$ K) estimated for free Sm^{3+} ions.[20] In Fig. 4(a) the deviation from the fit is observed above 200 K, which may be explained as a result of thermal population of the second excited multiplet ($J = 9/2$).

As seen from Fig. 4(b), occurrences of ferrimagnetic transitions are observed at T_{M2} and T_{M3} in the $\chi - T$ curve: These anomalies correspond well to the anomalies observed in the C_p-T and the ρ-T curves. On the other hand, the anomaly at T_{M1} is not clearly seen in the $\chi - T$ curve measured at 10 Oe.

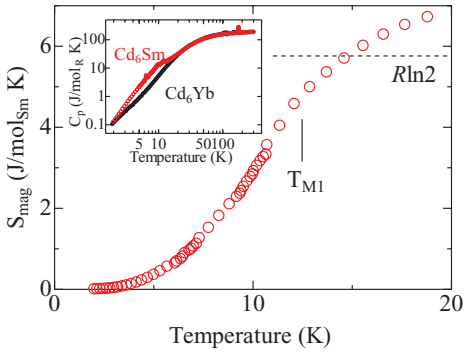

FIG. 5. (Color online) Magnetic entropy S_{mag} of Cd_6Sm obtained from subtracting the heat capacity of the nonmagnetic isostructural Cd_6Yb from that of Cd_6Sm shown in the inset. The magnetic entropy is shown in a range below 20 K since no appreciable difference is observed between the two compounds above ~20 K.

However, a close examination of the $\chi - T$ curve measured at 1000 Oe shown in the inset of Fig. 4(b) reveals that a slight decrease, i.e., an inflection, occurs around 12.5 K implying an occurrence of antiferromagnetic transition at T_{M1}. We note that the observation of ferrimagnetic transitions in crystalline approximants is reported for the first time in the present article.

Figure 5 shows the magnetic entropy S_{mag} of Cd_6Sm estimated by subtracting the specific heat of nonmagnetic isostructural Cd_6Yb from that of Cd_6Sm. Since the magnetic contribution to specific heat is observed only below ~20 K in the range 2−300 K (as seen in the inset), S_{mag} below 20 K is zoomed in within the figure. It is seen that S_{mag} reaches $\sim R$ ln2 at $T_{M1} = 12.5$ K, which is far less than the saturated value of the Hund's law ground state Sm^{3+} (R ln6). Since the site symmetry of Sm ions above $T_c = 179$ K is m, the sixfold degenerate Sm^{3+} $J = 5/2$ multiplet splits into three doublets under the crystalline electric field (CEF) above and, hence, below T_c. Thus, the obtained entropy of $\sim R$ ln2 at T_{M1} means that the ground state for the Sm^{3+} ions is a Kramers doublet, and the occurrence of the successive magnetic transitions in Cd_6Sm is understood as a consequence of a number of almost degenerated states for localized spins on the icosahedral cluster. Furthermore, no Schottky anomaly is observed above T_{M1}, which implies that the next higher CEF level is at a considerably higher energy, i.e., above 600 K, and its contribution is negligible in the studied temperature range.

Figure 6 shows the field dependence of magnetization measured for the two ferrimagnetic and the antiferromagnetic phases as well as for the paramagnetic one. Hysteresis due to the occurrences of spontaneous magnetization is clearly noticed in the M-H curves at 9 and 4.5 K, whereas those of the antiferromagnetic and paramagnetic phases, i.e., at 12 and 14 K, respectively, exhibit a linear dependence on the magnetic field with no hysteresis. The upper inset of Fig. 6 shows M-H curves at 4.5 and 2 K from 0 to 40 000 Oe. A metamagnetic anomaly is observed in both the M-H curves and the magnetic field of the anomaly increases from ~2500 to ~15 000 Oe with decreasing temperature, which is clear evidence that a ferrimagnetic order occurs at

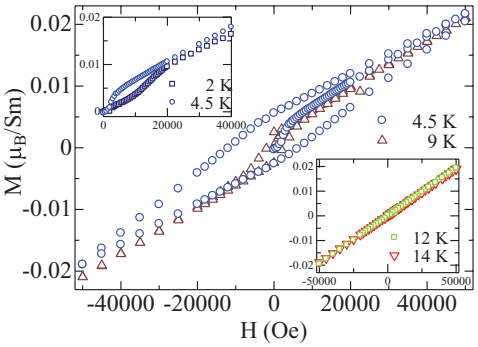

FIG. 6. (Color online) Magnetic field dependences of the magnetization M for the two ferrimagnetic phases of Cd_6Sm measured at 4.5 and 9 K. The lower inset shows those for the antiferromagnetic and paramagnetic ones measured at 12 and 14 K, respectively. Hysteresis is observed at 4.5 and 9 K, indicating occurrences of spontaneous magnetization. The upper inset shows M-H curves at 2 and 4.5 K from 0 to 40 000 Oe. A metamagnetic anomaly is noticed at ∼15 000 and ∼2500 Oe, respectively.

0 Oe below T_{M3}. For the influences of the magnetic transitions in the resistivity, the significant decrease of the resistivity on cooling from ∼10.2 K is attributed to a loss of scattering due to the ferrimagnetic transition at T_{M2}. On the other hand, the influence of the ferrimagnetic transition at T_{M3} in the resistivity is very weak and only a slight reduction of the resistivity is noticed, as is recognized in the $d\rho/dT$ curve, suggesting that a long-range magnetic order is mostly established at T_{M2}.

Now we discuss the ferrimagnetic structures of Cd_6Sm based on the low temperature superstructure.[21] Table I shows the character table of the small group G_k of the space group $C2/c$ for the propagation vector $k = (000)$. Among the four irreducible representations (irreps) of the small group, the spontaneous magnetization is described by the basis of the Γ_1 or Γ_3 irreps since a magnetic moment is invariant under the inversion operation. Then, the resulting magnetic space group is either $C2/c$ or $C2'/c'$, respectively.

TABLE I. Character table of the irreducible representations of the small group G_k of the space group $C2/c$ for the propagation vector $k = (0, 0, 0)$.

	$\{E \mid 000\}$	$\{C_{2y} \mid 0\,0\,1/2\}$	$\{I \mid 000\}$	$\{\sigma_y \mid 0\,0\,1/2\}$
Γ_1	1	1	1	1
Γ_2	1	1	−1	−1
Γ_3	1	−1	1	−1
Γ_4	1	−1	−1	1

In the case of $C2/c$, a net magnetic moment is parallel to the b-axis of the $C2/c$ lattice, whereas in the case of $C2'/c'$ the net moment lies inside the (a,c)-plane. In summary the ferrimagnetic transitions of Cd_6Sm have shown that a (pseudo) icosahedron made of localized spins can have a nonzero net magnetic moment for the first time.

IV. CONCLUSION

We have observed structural and magnetic transitions in the crystalline approximant Cd_6Sm. A structural phase transition occurs at $T_c = 179$ K, which is interpreted as a result of orientational ordering of the Cd_4 tetrahedron located at the center of the icosahedral cluster. Three successive magnetic transitions are found at $T_{M1} = 12.5$, $T_{M2} = 10.2$, and $T_{M3} = 6.5$ K. The transition at T_{M1} is attributed to an antiferromagnetic transition, and those at T_{M2} and T_{M3} are attributed to ferrimagnetic ones, which for the first time shows that an icosahedron made of localized spins can have a nonzero net magnetic moment, and the moments of the magnetic clusters form a long-range magnetic order.

ACKNOWLEDGMENTS

This work was supported by KAKENHI (Grant No. 20045017) from the ministry of Education, Culture, Sports, Science Technology of Japan.

*tamura@rs.noda.tus.ac.jp

[1] G. Bruzzone, M. L. Fornasini, and F. Merlo, J. Less-Common Met. **30**, 361 (1973).
[2] C. P. Gómez and S. Lidin, Phys. Rev. B **68**, 024203 (2003).
[3] S. Y. Piao, C. P. Gómez, and S. Lidin, Z. Naturforsch., B: Chem. Sci. **61b**, 644 (2006).
[4] A. P. Tsai, J. Q. Guo, E. Abe, H. Takakura, and T. J. Sato, Nature **408**, 537 (2000).
[5] J. Q. Guo, E. Abe, and A. P. Tsai, Phys. Rev. B **62**, R14605 (2000).
[6] R. Tamura, Y. Murao, S. Takeuchi, M. Ichihara, M. Isobe, and Y. Ueda, Jpn. J. Appl. Phys., Part 2 **41**, L524 (2002).
[7] R. Tamura, K. Edagawa, Y. Murao, S. Takeuchi, K. Suzuki, M. Ichihara, M. Isobe, and Y. Ueda, J. Non-Cryst. Solids **334-335**, 173 (2004).
[8] R. Tamura, K. Edagawa, C. Aoki, S. Takeuchi, and K. Suzuki, Phys. Rev. B **68**, 174105 (2003).
[9] R. Tamura, K. Edagawa, C. Aoki, S. Takeuchi, and K. Suzuki, J. Alloys Compd. **378**, 290 (2004).
[10] K. Nishimoto, R. Tamura, and Shin Takeuchi, Phys. Rev. B **81**, 184201 (2010).
[11] R. Tamura, K. Nishimoto, S. Takeuchi, K. Edagawa, M. Isobe, and Y. Ueda, Phys. Rev. B **71**, 092203 (2005).
[12] R. Tamura, K. Edagawa, K. Shibata, K. Nishimoto, S. Takeuchi, K. Saitoh, M. Isobe, and Y. Ueda, Phys. Rev. B **72**, 174211 (2005).
[13] T. Ishimasa, Y. Kasano, A. Tachibana, S. Kashimoto, and K. Osaka, Philos. Mag. **87**, 2887 (2007).
[14] T. Yamada *et al.* (unpublished).
[15] K. Nishimoto *et al.* (unpublished).
[16] R. Tamura, Y. Muro, T. Hiroto, K. Nishimoto, and T. Takabatake, Phys. Rev. B **82**, 220201 (2010).
[17] T. Yamada, R. Tamura, Y. Muro, K. Motoya, M. Isobe, and Y. Ueda, Phys. Rev. B **82**, 134121 (2010).
[18] W. M. Yuhasz, N. A. Frederick, P. C. Ho, N. P. Butch, B. J. Taylor, T. A. Sayles, M. B. Maple, J. B. Betts, A. H. Lacerda, P. Rogl, and G. Giester, Phys. Rev. B **71**, 104402 (2005).
[19] H. C. Hamaker, L. D. Woolf, H. B. MacKay, Z. Fisk, and M. B. Maple, Solid State Commun. **32**, 289 (1979).
[20] J. H. Van Vleck, *The Theory of Electric and Magnetic Susceptibilities* (Oxford University Press, London, 1932).
[21] Yu. A. Izyumov and V. E. Naish, J. Magn. Magn. Mater. **12**, 239 (1979).